Protonation of Gly_n Homologues in Matrix-Assisted Laser Desorption Ionization

Zohra Olumee and Akos Vertes*

Department of Chemistry, The George Washington University, Washington, D.C. 20052

Received: February 12, 1998; In Final Form: May 8, 1998

Protonation reactions of Gly_n homologues were studied in order to elucidate the effect of peptide chain length and matrix materials on the matrix-assisted laser desorption ionization (MALDI) mechanism. At 337 nm nitrogen laser excitation the relative ion yield–chain length relationship showed considerable variability in 3,5-dimethoxy-4-hydroxycinnamic acid (SA), 2,5-dihydroxybenzoic acid (DHB), 6-aza-2-thiothymine (ATT), and α-cyano-4-hydroxycinnamic acid (CHCA), the four matrices studied. For SA and ATT, a monotonic increase of relative ion yields (RIYs) was observed with increasing peptide length. Similar increasing pattern and significantly higher RIYs were found for the homologues of the Gly_n series in the CHCA matrix with the exception of Gly. The particularly high MALDI ion yield of this amino acid in CHCA may be attributed to preferential embedding and/or more efficient condensed-phase proton transfer. To unveil the nature of the proton-transfer reactions in MALDI, the peptide length dependence of the measured RIYs was compared to the trends observed in proton affinities (PAs) of the same homologues as well as to ion–molecule reaction rates calculated using the Langevin cross section. Chain extension enhancements in MALDI RIYs of *all* the studied matrices cannot be explained either by the increase in ground-state ion–molecule reaction rates or by a linear dependence on gas-phase PAs. However, in SA and ATT positive correlation was observed between MALDI RIYs of Gly_n homologues and their PAs. The RIYs observed in CHCA were significantly higher than in SA. This effect could be explained by the markedly lower PA of CHCA (183 ± 2 kcal/mol) compared to that of SA (204 ± 4 kcal/mol).

Introduction

The protonation of proteins accounts for most of the ionization reactions in matrix-assisted laser desorption ionization (MALDI) and in electrospray ionization (ESI). Mechanistic studies of these reactions have been hampered by the presence of abrupt competitive phase transitions in both MALDI and ESI. There are a number of possible pathways for proton transfer from the matrix to the guest molecule in the MALDI process: (a) solid-phase ground-state mechanism involving proton tunneling along hydrogen bonds, (b) solid-phase proton transfer from excited host species, (c) excited-state proton transfer (ESPT) in host–guest clusters during the desorption event, (d) ESPT in the gas phase, and (e) gas-phase proton transfer via ion–molecule reactions. Given the complexity of the system, this by no means is a complete list but represents the most commonly cited possibilities.

Although several groups have been trying to unveil the "true" mechanism of MALDI ionization, a definitive picture has not emerged. Russell and co-workers focused on the possible role of ESPT in the gas phase.[1] They pointed out that the gas-phase and especially the excited-state acidity of the protonated matrix molecule may be very different from the value we assign based on chemistry in aqueous solutions. Studying para-substituted aniline compounds as matrices, they concluded that the carboxyl hydrogen, common to the most efficient UV MALDI matrices, is not necessarily the source of the transferred proton.

Hillenkamp and co-workers advocated a complex multipath ionization mechanism based on gas-phase proton transfer from the protonated matrix molecule, [M+H]$^+$, and/or from the

matrix radical cation, M$^{\bullet+}$, to the protein species.[2] The contribution of the different reaction channels in this mechanism heavily depended on the laser wavelength and on the yield of the two possible initiating species.

Vertes and Gijbels modified the simple ion–molecule reaction theory[3] to predict proton-transfer rates in gas-phase collisions between a small matrix ion and a much larger molecule.[4] According to this kinetic theory the rate constants, and thus, assuming pseudo-first-order rate law, the abundances of the protonated protein molecules, are proportional to the square root of the protein polarizability, α:

$$k = 2\pi e(\alpha/m)^{1/2} \tag{1}$$

where m is the mass of the matrix ion. Since the polarizability of a molecule is roughly proportional to its volume, eq 1 predicts that larger proteins have higher ionization efficiencies. This increase in efficiency, however, diminishes at higher masses. More accurate predictions are possible based on more advanced theories of ion–molecule reactions that account for ion–permanent dipole interactions (e.g., the average dipole orientation theory, ADO).[5,6] Due to the sizable permanent dipole moment of zwitterionic protein species, ion–dipole interactions can be especially important if this form participates in the reaction. An obvious shortcoming of the pure ion–molecule reaction approach is the neglect of the reactants' chemical structure. In other words, the reactants are represented by their masses, polarizabilities, and charges only.

To investigate the chemical contribution of the guest molecule, in an earlier study we explored the dependence of MALDI ion yield on the amino acid composition of small peptides. It was observed that the presence of basic residues in peptides

* Corresponding author. Tel (202) 994-2717, Fax (202) 994-5873, E-mail vertes@gwu.edu.

Protonation of Gly$_n$ Homologues

J. Phys. Chem. B, Vol. 102, No. 31, 1998 **6119**

greatly enhanced the efficiency of protonation, and their absence resulted in moderate ion signals.[7] Chen and co-workers also reported that the detection of proteins or peptides was facilitated by the presence of a basic amino acid residue.[8]

In the case of peptides and proteins found in nature, the size-related effects and the effects related to the chemical nature of the residues cannot be isolated. To separate the chemical factors from size-related contributions, we decided to focus on homologue peptides differing only in length. Among the 20 common amino acids, glycine, Gly, is the simplest residue, making the Gly$_n$ homologues good candidates to study the role of the peptide size in ion formation. An additional advantage of this system is the availability of structural and thermochemical information for related species.

Structure and stability of Gly and Gly methyl complexes with H$^+$, Li$^+$, and Na$^+$ were studied using ab initio calculations.[9] The results of this investigation indicated that the favored protonation sites are the amino nitrogen and the carboxyl oxygen. To model the mass spectral behavior of singly and doubly protonated tetraglycine, Vekey and Gomory conducted semiempirical (MNDO) and ab initio (3-21G) calculations. The N-terminus was found to be the preferred site of protonation in singly charged tetraglycine.[10]

Gas-phase basicities (GB) and sites of protonation of glycine oligomers were studied by several other groups.[11-14] Wu and Lebrilla used semiempirical AM1 calculations along with bracketing measurements to determine site of protonation and GB of Gly$_n$ oligomers ($n = 1-5$). They concluded that the increase in GB between Gly and Gly$_2$ is due to the increased hydrogen-bonding interaction by the additional amide group.[11] To probe the effects of alkyl side chain on proton-transfer reactions, the same group also determined GBs for Gly, Ala, and Val. They found that the dipeptide had higher GB than the corresponding amino acid by ~3%, and in the case of Gly$_3$ this trend continued. No further increase was encountered as the peptide chain was extended to five amino acid residues.[12]

To determine GBs, Cassady and co-workers used ab initio Hartree−Fock molecular orbital calculations on Gly, Gly$_2$,[13] and Gly$_3$.[14] They too concluded that the most favorable sites of protonation in Gly were the amino nitrogen and the carboxylic carbonyl oxygen. In addition to these positions in Gly$_2$, two other sites, the amide nitrogen and the carbonyl oxygen in the peptide bond, were amenable to protonation.[13] In Gly$_3$ the following order was suggested for protonation propensities: amino N > amide carbonyl O > carboxylic carbonyl O > amide N.[14]

GBs and proton affinities (PAs) of small peptides can be determined by measuring the relative dissociation rates of dimer ions, also known as the "kinetic method".[15-19] The effects of the chain length on GBs and PAs of polyglycines were investigated by Wu and Fenselau using amines as standard reference. This group concluded that the PA of Gly$_n$ homologues in the $n = 1-10$ range increases as the number of residues increase by a total of ~15%.[16]

Ion formation in MALDI is thought to be a complex set of processes including the embedding of guest molecules into the matrix, as well as proton-transfer reactions in the solid and/or gas phase. Although there are strong variations in MALDI ion yields as a function of primary and secondary protein structure, no comprehensive information is available on the factors influencing ion production. In this study of ionization efficiencies, our main objective was to explore the effect of peptide chain length, peptide polarizability, peptide PA, and matrix material. Thus, a systematic investigation of relative ion yields

(RIYs) was carried out on Gly$_n$ homologues in the $n = 1-6$ range using different matrices. These results were compared to ion−molecule reaction rate calculations and to trends in experimental PAs.

Experimental Section

Instrumentation. A modified linear time-of-flight mass spectrometer (TOF 101, Comstock Inc., Oak Ridge, TN) was used to investigate the MALDI ion yields of Gly$_n$ homologues. Ion generation was accomplished by a nitrogen laser at 337 nm (VSL-337ND, Laser Science Inc., Newton, MA). Detailed description of the system can be found elsewhere.[7] Briefly, the MALDI-generated ions were accelerated to 10−30 kV and ejected into the field-free region of a time-of-flight (TOF) mass spectrometer. The ions were detected by a dual-microchannel plate (Galileo Electro-Optics Co., Sturbridge, MA) that was biased to 1900 V. The ion currents were amplified (×10) and recorded by a 200 MHz transient recorder (TR8828D, LeCroy, Albuquerque, NM). Further processing of the data was carried out using a custom-made data acquisition package (Tofware, Version 2.1, Ilys Software, Pittsburgh, PA) and a scientific data analysis package (Origin MicroCal Software, Inc., Northampton, MA). On our TOF system in the relevant mass range the typical mass resolution and mass accuracy were ~400 and 0.01%, respectively. Thus, even for the largest studied ion, the protonated hexaglycine, at m/z 361.32 unit mass resolution and easy identification were achieved.

Sample Preparation. The Gly$_n$ guest compounds were purchased from Sigma (St. Louis, MO). Guest solutions of 5.0 × 10^{-3} M concentration were freshly prepared every day in 1−5% trifluoroacetic acid (TFA). 3,5-Dimethoxy-4-hydroxy-cinnamic acid (sinapinic acid, SA, Aldrich, Milwaukee, WI), α-cyano-4-hydroxycinnamic acid (CHCA), 2,5-dihydroxyben-zoic acid (DHB), and 6-aza-2-thiothymine (ATT) (Sigma, St. Louis, MO) were used as matrices throughout the study. Saturated solutions of each matrix (~0.05 M) were prepared in 7:3 (v/v) mixture of HPLC grade acetonitrile and deionized water. Two microliter aliquots of the analyte were mixed with 10 μL of the matrix solution on the probe tip. The samples were dried in a stream of ambient air prior to insertion into the mass spectrometer (dried-drop method).

Spectrum Collection and Analysis. Due to the characteristics of the dried-drop method, the crystalline layer on the probe surface was heterogeneous and unevenly distributed. Therefore, significant shot-to-shot variations were observed in the signal intensity.[20] To eliminate the influence of laser power on RIYs, the laser irradiance corresponding to the ionization threshold for Gly was determined and used for every member of the Gly$_n$ series.

To improve shot-to-shot reproducibility and spot-to-spot repeatability and minimize the effect of variations in sample preparation, five samples were prepared for each matrix−analyte combination. Spectra were collected from eight randomly selected spots on the probe tip, and ~20 consecutive shots were collected from each spot. Thus, a database was generated in which 800 spectra were accumulated for every homologue. From these sets only spectra with overloaded or missing matrix peaks were discarded (<20%). To improve the signal-to-noise ratio, from the remaining data 15 sets of 20 consecutive spectra were averaged. The raw ion current data were analyzed using the Origin scientific graphics package. The areas under the ion current peaks were determined using Gaussian fit that appeared to best represent the data in the mass range of interest. RIYs
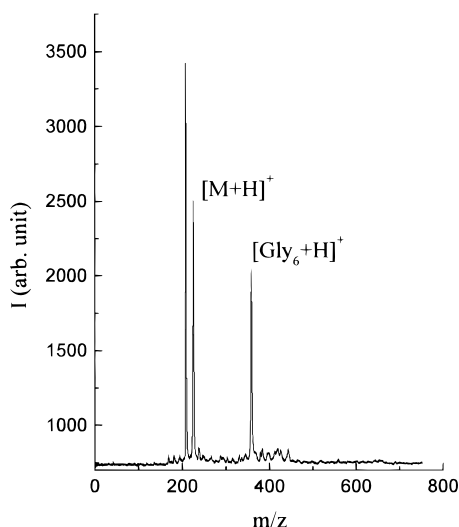
Figure 1. MALDI mass spectrum of Gly_6 in sinapinic acid matrix. The protonated matrix molecule, $[M+H]^+$, and the protonated hexaglycine, $[Gly_6+H]^+$, are clearly distinguished.
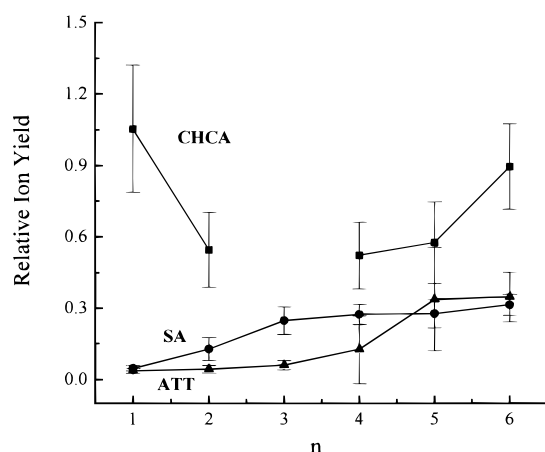
Figure 2. RIYs of Gly_n homologues using three different matrices at $\lambda = 337$ nm. The missing point on the CHCA curve is the result of matrix interference with the Gly_3 data.

were expressed as the peak area ratio of protonated analyte and matrix molecules.

Results and Discussion

Initially we selected SA, ATT, CHCA, and DHB as matrices because they had been extensively used for MALDI of peptides. After the preliminary experiments, DHB was excluded from the study because of its tendency to form large (1−2 mm) needle-shaped crystals aggregated at the rim of the probe. This crystallization pattern resulted in large ion intensity fluctuations due to the uneven coverage of the probe surface. A typical MALDI mass spectrum for Gly_6 in SA is shown in Figure 1. The protonated matrix and guest molecules were readily identified.

For the SA, ATT, and CHCA the determined RIYs showed considerable variations as a function of chain length and matrix material (see Figure 2). Using SA and ATT matrices, the intensities of protonated guest molecules became more abundant as the number of residues increased. In CHCA matrix, the increasing trend of ion yields did not hold valid for the first two homologues, but it prevailed for the $n = 4-6$ members of the series. The relative ion intensities in this matrix were 0.5−1 order of magnitude higher than for the other two matrices. For

TABLE 1: Langevin Rate Constants, k, and RIYs for Gly_n Homologues in Three Different Matrices

matrix ion	guest	μ $(10^{-22}$ g)	α^a $(10^{-23}$ cm$^{-3})$	k $(10^{-10}$ cm^3/s)	RIY
$[SA+H]^+$	Gly	0.93	0.65	7.97	0.047
	Gly_2	1.38	1.16	8.74	0.127
	Gly_3	1.71	1.67	9.44	0.248
	Gly_4	1.95	2.18	10.1	0.275
	Gly_5	2.15	2.69	10.7	0.277
	Gly_6	2.3	3.21	11.3	0.314
$[CHCA+H]^+$	Gly	0.89	0.65	8.15	1.05
	Gly_2	1.29	1.16	9.03	0.547
	Gly_3	1.58	1.67	9.83	N/A
	Gly_4	1.78	2.18	10.6	0.522
	Gly_5	1.94	2.69	11.2	0.576
	Gly_6	2.07	3.21	11.9	0.895
$[ATT+H]^+$	Gly	0.82	0.65	8.51	0.035
	Gly_2	1.15	1.16	9.61	0.043
	Gly_3	1.36	1.67	10.6	0.06
	Gly_4	1.51	2.18	11.5	0.125
	Gly_5	1.62	2.69	12.3	0.347
	Gly_6	1.71	3.21	13.1	0.347

^{a} Values were calculated according to ref 22.

Gly in CHCA an extremely strong peak was detected at $m/z = 76.1$ (presumably corresponding to the protonated molecule of Gly). This observation was profoundly different from results in the other two matrices (SA and ATT) that produced weak responses for Gly under the same conditions. Testing a blank matrix sample confirmed that this signal was not related to the fragmentation of CHCA.

Since sample preparation and laser parameters were kept strictly unchanged between the runs, it is reasonable to assume that the generated species and their number densities in the plume are similar for the different homologues. Thus, in the case of a pseudo-first-order reaction between the protonated matrix molecules and the different peptides, the RIYs of protonated peptide molecules may be directly related to the different reaction rates. Considering thermal conditions and small reactants, gas-phase protonation reaction rates can be estimated using the angular momentum corrected average dipole orientation (AADO) theory:[3,5,21]

$$k_{AADO} = \frac{2\pi q\alpha^{1/2}}{\mu^{1/2}}\left[1 + C\frac{\mu_D}{\alpha^{1/2}}\left(\frac{2}{\pi kT}\right)^{1/2} + Z\mu_D\frac{I^{1/2}}{\alpha^{3/4}}\right] \quad (2)$$

where μ is the reduced mass of the system, whereas q, μ_D, and I denote the charge, the dipole moment, and the moment of inertia of the reactants, respectively. The C dipole locking constants and the Z angular momentum parameters are tabulated for different T temperatures.[5,21] The first term of eq 2 coincides with the prediction of the Langevin theory. Evaluation of the Langevin rate constants for the possible ground-state proton-transfer reactions is summarized in Table 1. The molecular polarizabilities of the peptides are estimated using the updated semiempirical atomic hybridization polarizability method.[22] Comparing the normalized RIYs and Langevin rate constants in Figure 3, it is obvious that in this approximation the significant RIY enhancement for higher homologues cannot be explained by higher protonation rates alone.

In the case of molecules with permanent dipole moments, better rate constant estimates could be obtained by evaluating the second and third terms of eq 2. Among the possible forms of Gly_n, the zwitterionic species are likely to have substantial dipole moments. For example, the measured dipole moment values of zwitterionic glycine are in the 11.6−15.7 D range.[23] Although studies of isolated Gly molecules indicate that they

Protonation of Gly$_n$ Homologues

J. Phys. Chem. B, Vol. 102, No. 31, 1998 **6121**
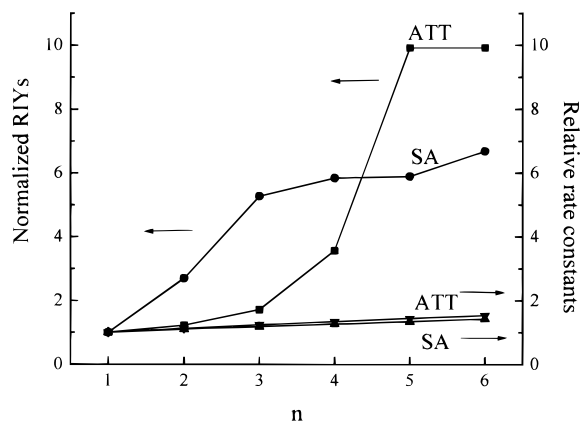
Figure 3. RIYs and Langevin ion−molecule reaction rate constants for Gly$_n$ homologues normalized for Gly in SA and ATT matrices.

TABLE 2: RIYs in SA, Proton Affinities, and Gas-Phase Basicities of Polyglycine, Gly$_n$

n	RIY^a	PA^b (kcal/mol)	PA^d (kcal/mol)	GB^c (kcal/mol)	GB^d (kcal/mol)
1	0.047 ± 0.01	211.6	211.8	206.2 ± 2.2	203.7
2	0.127 ± 0.05	219.1 ± 0.8	N/A	215.3 ± 2.5	210.8
3	0.248 ± 0.06	223.1 ± 0.5	231.1	218.9 ± 2.9	219.1
4	0.275 ± 0.04	227.2 ± 0.4	232.7	225.0 ± 2.3	221.8
5	0.277 ± 0.06	231.8 ± 0.7	N/A	225.3 ± 4.4	220.1
6	0.314 ± 0.04	234.4 ± 0.6	N/A	227.4 ± 4.6	227.1

^{a} RIY is the ratio of protonated analyte and matrix ion intensities measured in SA at 337 nm. ^{b} From ref 16. ^{c} Experimental values from ref 13. ^{d} These are the latest reconciled values from the NIST WebBook (see ref 12).

are not in zwitterionic form in the gas phase,[24,25] high-level ab initio studies confirm that the zwitterionic form becomes much more favored in polar condensed-phase environments[26] (e.g., water, matrix crystal). Thus, it is probable that the Gly$_n$ species are embedded as zwitterions in the polar matrix crystals, and it is conceivable that they preserve this structure throughout some part of the desorption event (partially stabilized by nearby MH$^+$ ions). Based on extrapolating the data in Figure 1 of ref 5, the C dipole locking constant for a molecule with larger than 4 D dipole moment exceeds 0.26. Using this value, one can express the lower limit for the contribution of the dipole term, i.e., the second term in eq 2, as 5.6 times the first term. Since no zwitterionic dipole moments are available for the higher Gly$_n$ homologues, the related rate enhancement effects cannot be evaluated. The third term of eq 2 introduces an additional size-related effect, namely, the increase in the reaction rate constant with the net increase of $I/\alpha^{1/2}$. This enhancement is likely to play a significant role in the case of bulky proteins.

Russell and co-workers demonstrated the correlation between guest ion yields and the gas-phase acidity of the matrix.[1] As a corollary to this finding, we were interested in exploring the relationship between proton-accepting properties of the guest molecules and their RIYs. In the case of SA and ATT matrices we found a clear positive correlation between the MALDI ion yields of Gly$_n$ homologues and their PAs measured by the kinetic method. The PA and GB values were obtained from refs 12, 13, and 16 and listed in Table 2. Significant correlation was found between the RIY and the PA data for the Gly$_n$ series in SA matrix with a regression coefficient of $R = 0.95$ (Figure 4), whereas for ATT $R = 0.88$ was observed. In the case of CHCA, however, this correlation was absent possibly due to the differences in embedding, absorption, excitation, and internal conversion steps preceding the proton transfer.
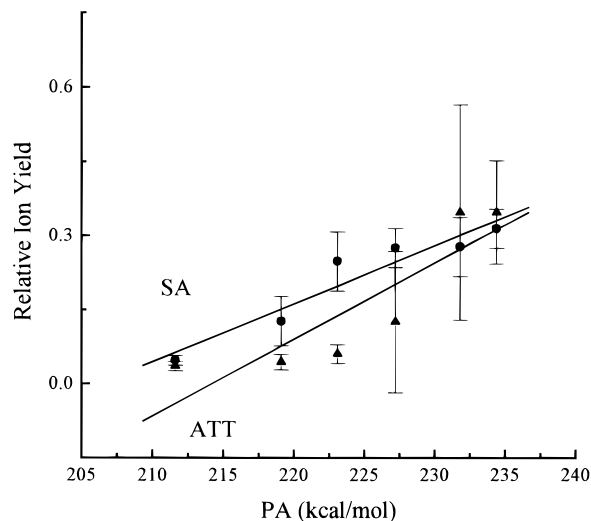
Figure 4. Correlation of MALDI RIYs for Gly$_n$ homologues and PAs obtained by the kinetic method using FAB ion source. Linear regression coefficients for SA and ATT are 0.95 and 0.88, respectively.

In the following section we argue that for these matrices there may be a competition between protonation from the ground state and protonation from the excited state. The relative populations of these two states at any given laser irradiance depend on the solid-phase absorption coefficient of the matrix at the laser wavelength and on the energy required for the transition. Dyer and co-workers measured the UV absorption spectrum of several matrices in thin-film form.[27] At 337 nm excitation the absorption coefficient of CHCA ($\alpha_{337\ nm} = 2.2 \times 10^5$ cm^{-1}) was found to be a factor of 2 higher than the absorption coefficient of SA ($\alpha_{337\ nm} = 1.1 \times 10^5$ cm^{-1}) under the same laser irradiance. At the same time, comparing the absorption maxima between 300 and 400 nm revealed that λ_{max} for SA was slightly blue-shifted. Both of these factors point to a more populated excited state in the case of CHCA. Thus, the significantly higher RIYs in CHCA can be explained by the contribution of a reaction channel via excited matrix species.

An alternative explanation of this effect is based on PA values measured for the matrices. Recent bracketing experiments have shown markedly lower PA for CHCA (183 ± 2 kcal/mol) than for SA (204 ± 4 kcal/mol).[28] One can argue that proton transfer from the ground state of the protonated CHCA species to Gly$_n$ occurs more readily than from protonated SA due to the ~21 kcal/mol advantage in the PA balance.

There are two possibilities to rationalize the dramatically higher RIY for Gly in CHCA matrix. A proton-transfer reaction may take place in the condensed phase between the analyte and the matrix that leads to enhanced [Gly+H]$^+$ ion signal intensity. The other possible explanation may be related to the preferential embedding of Gly into the matrix. In other words, a better cocrystallization and more efficient incorporation of the guest molecules into the host crystal may lead to higher desorption and consequently higher ion yields.

In conclusion, with the exception of Gly in CHCA, all the other homologues showed an increasing pattern of RIYs as a function of peptide length. This behavior maybe generalized to other proteins and may explain high ion yields from this class of biomolecules. Increasing the length of polypeptides with different residues opens other possibilities for preferential ionization. The appearance of secondary and tertiary structure determines which residues are exhibited at the outer surface of the molecule. Thus, conformations with basic residues exposed can undergo protonation with higher probability.

References and Notes

(1) Gimon-Kinsel, M.; Preston-Schaffter, L.; Kinsel, G.; Russell, D. *J. Am. Chem. Soc.* **1997**, *119*, 2534.

(2) Ehring, H.; Karas, M.; Hillenkamp, F. *Org. Mass Spectrom.* **1992,** *27*, 472.

(3) Gioumousis, G.; Stevenson, D. P. *J. Chem. Phys.* **1958**, *29*, 294.

(4) Vertes, A.; Gijbels, R. In *Laser Ionization Mass Analysis*; Vertes, A., Gijbels, R., Adams, F., Eds.; John Wiley: New York, 1993; p 127.

(5) Bass, L.; Su, T.; Chesnavich, W. J.; Bowers, M. T. *Chem. Phys. Lett.* **1975**, *34*, 119.

(6) Hsieh, E. T. Y.; Castleman, A. W., Jr. *Int. J. Mass Spectrom. Ion Phys.* **1981**, *40*, 295.

(7) Olumee, Z.; Sadeghi, M.; Tang, X.; Vertes, A. *Rapid Commun. Mass Spectrom.* **1995**, *9*, 744.

(8) Zhu, Y.; Lee, K. L.; Tang, K.; Allman, S. L.; Taranenko, N. I.; Chen, C. H. *Rapid Commun. Mass Spectrom.* **1995**, *9*, 1315.

(9) Jensen, F. *J. Am. Chem. Soc.* **1992**, *114*, 9533.

(10) Vekey, K.; Gomory, A. *Rapid Commun. Mass Spectrom.* **1996**, 10, 1485.

(11) Wu, J.; Lebrilla, C. B. *J. Am. Chem. Soc.* **1993**, *115*, 3270.

(12) Hunter, E. P.; Lias, S. G. In *NIST Standard Reference Database Number 69*; Mallard, W. G., Linstrom, P. J., Eds.; National Institute of Standards and Technology: Gaithesburg, MD, Aug 1997 (http://web book.nist.gov).

(13) Zhang, K.; Zimmerman, D. M.; Chung-Phillips, A.; Cassady, C. J. *J. Am. Chem. Soc.* **1993**, *115*, 10812.

(14) Zhang, K.; Cassady, C. J.; Chung-Phillips, A. *J. Am. Chem. Soc.* **1994**, *116*, 11512.

(15) Wu, Z.; Fenselau, C. *Rapid Commun. Mass Spectrom.* **1992**, *6*, 403.

(16) Wu, Z.; Fenselau, C. *J. Am. Soc. Mass Spectrom.* **1992**, *3*, 863.

(17) Wu, Z.; Fenselau, C. *Tetrahedron* **1993**, *49*, 9197.

(18) Wu, Z.; Fenselau, C. *Rapid Commun. Mass Spectrom.* **1994**, *8*, 777.

(19) Gorman, G. S.; Spier, J. P.; Turner, C. A.; Amster, I. J. *J. Am. Chem. Soc.* **1992**, *114*, 3986.

(20) Salehpour, M.; Perera, I.; Kjellberg, J.; Hedin, A.; Islamian, M. A.; Hakansson, P.; Sundqvist, B. U. R. *Rapid Commun. Mass Spectrom.* **1989**, *3*, 259.

(21) Su, T.; Su, E. C. F.; Bowers, M. T. *J. Chem. Phys.* **1978,** *69,* 2243.

(22) Miller, K. J. *J. Am. Chem. Soc.* **1990,** *112*, 8543.

(23) Abraham, R. J.; Hudson, B. *J. Comput. Chem.* **1985,** *6,* 173.

(24) Price, W. D.; Jockusch, R. A.; Williams, E. R. *J. Am. Chem. Soc.* **1997,** *119*, 11988.

(25) Price, W. D.; Jockusch, R. A.; Williams, E. R. *J. Am. Chem. Soc.* **1998,** *120*, 3474.

(26) Zheng, Y.-J.; Ornstein, R. L. *J. Am. Chem. Soc.* **1996,** *118*, 11237.

(27) Allwood, D. A.; Dreyfus, R. W.; Perera, I. K.; Dyer, P. E. *Rapid Commun. Mass Spectrom.* **1996**, *10*, 1575.

(28) Burton, R. D.; Watson, C. H.; Eyler, J. R.; Lang, G. L.; Powell, D. H.; Avery, M. Y. *Rapid Commun. Mass Spectrom.* **1997**, *11*, 443.